

# CCDWT-GAN: generative adversarial networks based on color channel using discrete wavelet transform for document image binarization

Rui-Yang Ju<sup>[0000–0003–2240–1377]</sup>, Yu-Shian Lin<sup>[0000–0001–9825–9958]</sup>, Jen-Shiun Chiang<sup>[0000–0001–7536–8967]</sup>, Chih-Chia Chen<sup>[0000–0003–0848–9747]</sup>, Wei-Han Chen<sup>[0009–0005–2805–219X]</sup>, and Chun-Tse Chien<sup>[0009–0008–7549–4021]</sup>

Tamkang University, New Taipei City, 251301, Taiwan  
 jryjry1094791442;abcpp12383;jsken.chiang;crystal88irene;kj211378@gmail.com  
 popper0927@hotmail.com

**Abstract.** To efficiently extract the textual information from color degraded document images is an important research topic. Long-term imperfect preservation of ancient documents has led to various types of degradation such as page staining, paper yellowing, and ink bleeding; these degradations badly impact the image processing for information extraction. In this paper, we present CCDWT-GAN, a generative adversarial network (GAN) that utilizes the discrete wavelet transform (DWT) on RGB (red, green, blue) channel splited images. The proposed method comprises three stages: image preprocessing, image enhancement, and image binarization. This work conducts comparative experiments in the image preprocessing stage to determine the optimal selection of DWT with normalization. Additionally, we perform an ablation study on the results of the image enhancement stage and the image binarization stage to validate their positive effect on the model performance. This work compares the performance of the proposed method with other state-of-the-art (SOTA) methods on DIBCO and H-DIBCO ((Handwritten) Document Image Binarization Competition) datasets. The experimental results demonstrate that CCDWT-GAN achieves a top two performance on multiple benchmark datasets, and outperforms other SOTA methods.

**Keywords:** Semantic segmentation · Discrete wavelet transform · Generative adversarial networks · Document image binarization

## 1 Introduction

Document image binarization is a hot research topic in computer vision. While the traditional binarization methods are capable of extracting textual information from regular document images, they often struggle to handle degraded ancient document images, including text degradation and bleed-through [15,29].

In recent years, image binarization methods based on deep learning have shown remarkable performance, solving the problems that traditional image binarization methods [18,17,26] cannot solve. Several methods have been proposed

and achieved state-of-the-art (SOTA) performance in degraded document image binarization, such as the conditional generative adversarial network-based method [33], the hierarchical deep supervised network [32], and the iterative supervised network [10], which all outperform traditional image processing methods and other deep learning-based methods.

The aforementioned image binarization methods primarily focus on grayscale document images, specifically black and white degraded ancient documents. Considering that some scanned images of ancient documents are in color, we propose CCDWT-GAN, a generative adversarial network (GAN) that utilizes the discrete wavelet transform (DWT) on RGB (red, green, blue) splitted images to binarize the color degraded documents.

This paper makes the following contributions:

- 1) Demonstrating that using DWT on RGB splitted images can improve the efficiency of the generator and the discriminator, which enhances the performance of the model and achieves a better balance between text detail extraction and background error suppression.
- 2) Presenting a novel method for document image binarization that achieves SOTA performance on multiple benchmark datasets.

The rest of this paper is organized as follows: Section 2 introduces the related work of document image binarization and GANs. Section 3 provides detailed information about the proposed method. Section 4 presents a quantitative comparison with SOTA methods on benchmark datasets. Finally, Section 5 concludes this paper and discusses the future work.

## 2 Related Work

There are two main categories of document image binarization methods: traditional image processing methods and semantic segmentation methods based on deep learning. The traditional image processing method involves binarizing the image by calculating a pixel-level local threshold [18,17,26]. On the other hand, the deep learning-based semantic segmentation method utilizes U-Net [25] to capture contextual and location information. It maps the input image through the encoder and decoder to obtain the binarized image [32,10].

Recently, GANs [7] have shown impressive success in generating realistic images. Zhao *et al.* [33] introduced a cascaded generator structure based on Pix2Pix GAN [12] for image binarization. This architecture effectively addresses the challenge of combining multi-scale information. Bhunia *et al.* [3] conducted texture enhancement on datasets and utilized conditional generative adversarial networks (cGAN) for image binarization. Suh *et al.* [27] employed Patch GAN [12] to propose a two-stage generative adversarial networks for image binarization. De *et al.* [4] developed a dual-discriminator framework that integrates local and global information. These methods all achieve the SOTA performance for document image binarization.

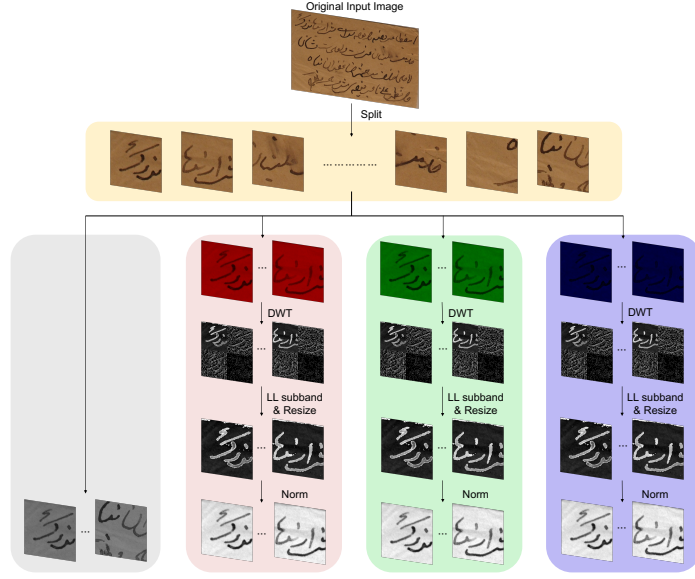


**Fig. 1.** The structure of the proposed model for image preprocessing. The original input image is split into multiple  $224 \times 224$  patches. The RGB channel splitted images retain LL subband after DWT, then resize to  $224 \times 224$  pixels, and perform normalization.

### 3 Proposed Method

This work aims to perform image binarization on color degraded documents. Due to the diverse and complex nature of document degradation, our method performs adversarial network on RGB splitted images and a grayscale image, respectively. The proposed method consists of three stages: image preprocessing, image enhancement, and image binarization.

#### 3.1 Image Preprocessing

The proposed method employs four independent generators to extract the foreground color information and eliminate the background color from the image. In order to obtain input images for four independent generators, we first split the RGB three-channel input image into three single-channel images and a grayscale image, as shown in Fig. 1. To preserve more information in the RGB channel splitted image, this work applies DWT to each single-channel image to retain the LL subband image, then resizes to  $224 \times 224$  pixels, and finally performs normalization. There are many options to process the input image of the generator and the discriminator, such as whether to perform normalization. In section 4.4, we conduct comparative experiments to find the best option.

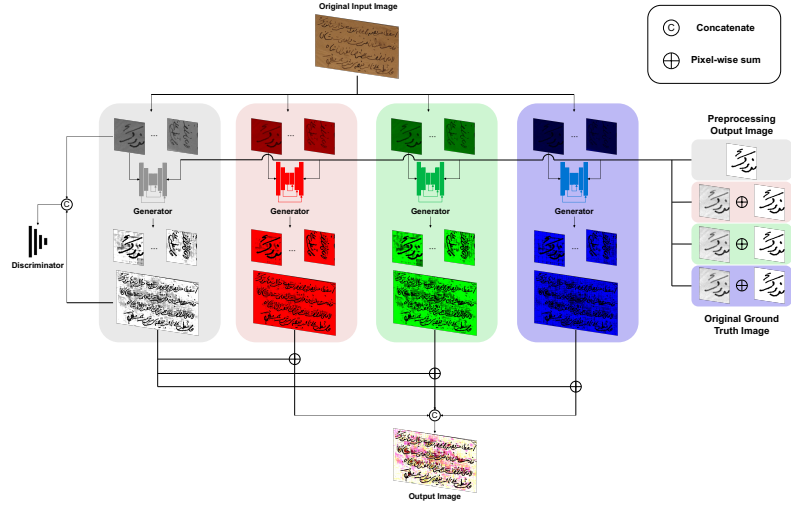


**Fig. 2.** The structure of the proposed model for image enhancement. The preprocessing output images and the original ground truth images are summed (pixel-wise) as the ground truth images of the generator.

### 3.2 Image Enhancement

In this stage, depicted in Fig. 2, the RGB three-channel input image is split into three single-channel images and a grayscale image. Each image utilizes an independent generator and shares the same discriminator to distinguish between the generated image and its corresponding ground truth image. The trained network is capable of eliminating background information from the local image patches and extracting color foreground information. Specifically, we employ U-Net++ [34] with EfficientNet [30] as the generator to extract features.

Due to the unpredictable degree of document degradation, four independent adversarial networks are used to extract text information from various color backgrounds, minimizing the interference caused by color during document image binarization. Since images with different channel numbers cannot be directly put into the same discriminator, the input of the discriminator requires a three-channel image, and the ground truth image is a grayscale (single-channel) image. As shown in the right of Fig. 2, the original ground truth image and the output image obtained from image preprocessing are summed at the pixel level to serve as the corresponding ground truth images.

### 3.3 Image Binarization

The proposed method employs a multi-scale adversarial network for generating images of local binarization and global binarization, enabling more accurate differentiation between the background and text. Moreover, we conduct global binarization on the original input images to offset any potential loss of spatial

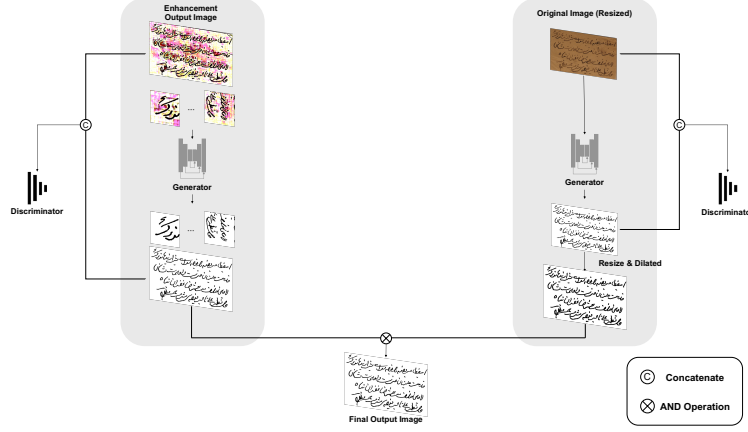


**Fig. 3.** The structure of the proposed model for image binarization. The input image size for the left generator is  $224 \times 224$  pixels, and for the right is  $512 \times 512$  pixels.

contextual information in the images caused by local prediction. Since the input image for local prediction in this stage is an 8-bit image, and the image binarization stage employs a 24-bit three-channel image, we employ two independent discriminators in the image binarization stage, respectively. As depicted in Fig. 3, the input image for local prediction (left) corresponds to the output of the image enhancement, while the input image size for global prediction (right) is  $512 \times 512$  pixels.

During the image binarization, the structure of the generator remains consistent with that of the image enhancement stage. As shown in the right of Fig. 3, when utilizing public datasets like DIBCO, the provided data include diverse scales document images, and we directly binarize the original input images by resizing them to the desired sizes ( $512 \times 512$ ).

### 3.4 Loss Function

In order to achieve a more stable convergence of the loss function, the proposed method utilizes the Wasserstein GAN [8] target loss function. The report of Bartusiak *et al.* [1] demonstrates that the binary cross-entropy (BCE) loss outperforms the L1 loss for binary classification tasks. Therefore, we utilize the BCE loss instead of the L1 loss employed in Pix2Pix GAN [12]. The Wasserstein GAN target loss function including the BCE loss is defined as follows:

$$\mathbb{L}_D = -\mathbb{E}_{x,y}[D(y,x)] + \mathbb{E}_x[D(G(x),x)] + \alpha \mathbb{E}_{x,\hat{y} \sim P_{\hat{y}}}[(\|\nabla_{\hat{y}} D(\hat{y},x)\|_2 - 1)^2] \quad (1)$$

$$\mathbb{L}_G = \mathbb{E}_x[D(G(x),x)] + \lambda \mathbb{E}_{G(x),y}[y \log G(x) + (1-y) \log(1-G(x))] \quad (2)$$

where the penalty coefficient is  $\alpha$ , and the uniform sampling along a straight line between the ground truth distribution  $P_y$  and the point pairs of the generated data distribution is  $P_{\hat{y}}$ .  $\lambda$  is used to control the relative importance of different loss terms. The parameter of the generator is  $\theta_G$  and the parameter of the discriminator is  $\theta_D$ . In the discriminator, the generated image is distinguished from the ground truth image by the target loss function  $\mathbb{L}_D$  in Eq. (1). In the generator, the distance between the generated image and the ground truth image in each color channel is minimized by the target loss function  $\mathbb{L}_G$  in Eq. (2).

## 4 Experiments

### 4.1 Datasets

This work trains the model on several public datasets and compares the performance of the proposed method with other SOTA methods on benchmark datasets. Our training sets include Document Image Binarization Competition (DIBCO) 2009 [6], Handwritten Document Image Binarization Competition (H-DIBCO) 2010 [19], H-DIBCO 2012 [21], Persian Heritage Image Binarization Dataset (PHIBD) [16], Synchromedia Multispectral Ancient Document Images Dataset (SMADI) [11], and Bickley Diary Dataset [5]. The benchmark test sets comprise DIBCO 2011 [20], DIBCO 2013 [22], H-DIBCO 2016 [23], and DIBCO 2017 [24].

### 4.2 Evaluation Metric

Four evaluation metrics are employed to evaluate the proposed method and conduct a quantitative comparison with other SOTA methods for document image binarization. The evaluation metrics utilized include F-measure (FM), Pseudo-F-measure (p-FM), Peak signal-to-noise ratio (PSNR), and Distance reciprocal distortion (DRD).

### 4.3 Experiment Setup

The backbone neural network of this work is EfficientNet-B6 [30]. This paper utilizes a pre-trained model on the ImageNet dataset to reduce computational costs. During the image preprocessing stage, we divide the input images into  $224 \times 224$  pixels patches, corresponding to the image size in the ImageNet dataset. The patches are sampled with scale factors of 0.75, 1, 1.25, and 1.5, and the images are rotated by  $0^\circ$ ,  $90^\circ$ ,  $180^\circ$ , and  $270^\circ$ . In total, the number of the training image patches are 336,702.

During the global binarization, we resize the original input image to  $512 \times 512$  pixels and generate 1,890 training images by applying horizontal and vertical flips. The input images for the local binarization of the image binarization stage are obtained from the image enhancement stage, and both stages share the same training parameters. The image binarization stage is trained for 150 epochs,

**Table 1.** Model performance comparison of different input images and different ground truth images of the generator. The performance of the proposed model is evaluated on (a) DIBCO 2011, (b) DIBCO 2013, (c) H-DIBCO 2016. Best and 2nd best performance are in red and blue colors, respectively.

(a) DIBCO 2011						
Option	Input	GT	FM $\uparrow$	p-FM $\uparrow$	PSNR $\uparrow$	DRD $\downarrow$
1	\	\	86.68	89.61	19.27	4.01
2	\	DWT (LL)	88.20	90.57	19.53	3.45
3	\	DWT (LL) + Norm	87.70	90.24	19.65	3.45
4	DWT (LL)	\	87.74	89.69	18.88	3.78
5	DWT (LL) + Norm	\	89.33	91.94	19.49	3.37
6	DWT (LL)	DWT (LL)	90.53	92.82	19.68	3.11
7	DWT (LL) + Norm	DWT (LL) + Norm	89.06	92.25	19.59	3.31
(b) DIBCO 2013						
Option	Input	GT	FM $\uparrow$	p-FM $\uparrow$	PSNR $\uparrow$	DRD $\downarrow$
1	\	\	92.94	94.70	21.57	2.74
2	\	DWT (LL)	94.43	95.64	21.79	2.13
3	\	DWT (LL) + Norm	94.88	96.19	22.32	1.95
4	DWT (LL)	\	93.23	94.43	20.80	2.67
5	DWT (LL) + Norm	\	93.76	95.41	21.54	2.40
6	DWT (LL)	DWT (LL)	94.39	95.34	21.91	2.26
7	DWT (LL) + Norm	DWT (LL) + Norm	94.55	95.86	22.02	2.07
(c) H-DIBCO 2016						
Option	Input	GT	FM $\uparrow$	p-FM $\uparrow$	PSNR $\uparrow$	DRD $\downarrow$
1	\	\	90.74	94.46	19.39	3.30
2	\	DWT (LL)	91.76	95.74	19.67	2.93
3	\	DWT (LL) + Norm	91.49	96.46	19.68	2.92
4	DWT (LL)	\	91.86	94.95	19.62	2.99
5	DWT (LL) + Norm	\	91.28	96.03	19.47	3.04
6	DWT (LL)	DWT (LL)	91.68	95.90	19.68	2.93
7	DWT (LL) + Norm	DWT (LL) + Norm	91.95	95.87	19.75	2.84

while the other stages are trained for 10 epochs each. This work utilizes the Adam optimizer with a learning rate of  $2 \times 10^{-4}$ .  $\beta_1$  of the generator and  $\beta_2$  of the discriminator are 0.5 and 0.999, respectively.

#### 4.4 Comparative Experiment

In this section, the performance of various options in the image preprocessing stage is compared. The benchmark datasets are used to evaluate the performance of model that utilizes UNet [25] with EfficientNet [30] as the generator. Three options are designed for the input images of the generator: direct input image,

**Table 2.** Ablation study of the proposed model on benchmark datasets.

Methods	Dataset	FM $\uparrow$	p-FM $\uparrow$	PSNR $\uparrow$	DRD $\downarrow$
Enhancement	DIBCO 2011	80.32	93.93	16.02	5.19
Proposed	DIBCO 2011	94.08	97.08	20.51	1.75
Enhancement	DIBCO 2013	86.19	97.36	17.91	3.81
Proposed	DIBCO 2013	95.24	97.51	22.27	1.59
Enhancement	H-DIBCO 2016	81.60	95.65	16.82	5.62
Proposed	H-DIBCO 2016	91.46	96.32	19.66	2.94
Enhancement	DIBCO 2017	78.76	93.30	15.15	5.84
Proposed	DIBCO 2017	90.95	93.79	18.57	2.94

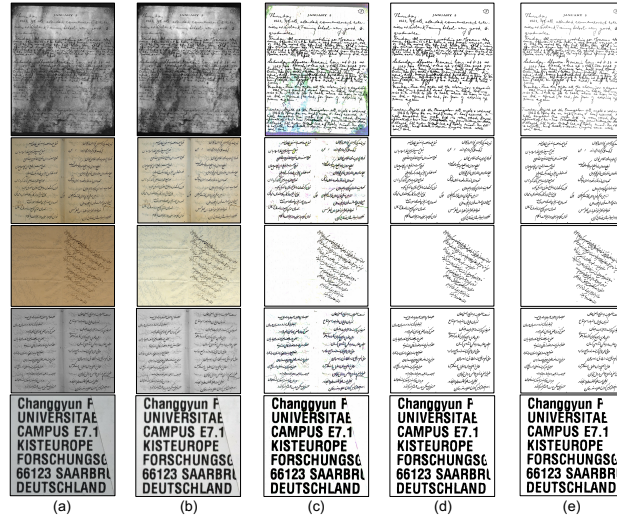
DWT to LL subband image, and DWT to LL subband image with normalization. Similarly, three options are set up for the ground truth images, which is the same as the input image.

Table 1 presents the performance of all options on the benchmark datasets. It can be seen that option 1, which directly uses the original image as input and discriminates between the directly generated image and the original ground truth image, exhibits the worst performance on all four datasets. On DIBCO 2011 dataset, option 6 achieves the best performance, which utilizes only the DWT without normalization as the input image, corresponding to the ground truth image. Option 3 achieves the top performance on DIBCO 2013 dataset by directly inputting the original image and utilizing the image processing output image as the corresponding ground truth. Moreover, option 3 achieves the top two performance in DIBCO 2016 dataset. Based on this, we choose option 3 to employ UNet++ [34] with EfficientNet [30] as the generator for network design.

#### 4.5 Ablation Study

In this section, this work presents an ablation study conducted to assess the individual contributions of each stage of the proposed method. We evaluate the output of the image enhancement stage, as “Enhancement”, and compare it with the final output, as “Proposed”. The evaluation and comparison of the output results are performed on four DIBCO datasets. Table 2 demonstrates that the output result of “Enhancement” is worse than the final output in terms of FM, p-FM, PSNR, and DRD values.

Section 4.4 demonstrates that training the generator after applying DWT and normalization enhances the model performance. However, it is important to further highlight the advantages of each stage. We choose five images from PHIBD [16] and Bickley Diary Dataset [5] to demonstrate the step-by-step output results of image enhancement and image binarization using the proposed method. Fig. 4 depicts the result denoted as (b), which corresponds to preserving the LL subband image after applying DWT and normalization. At this stage, noise reduction is performed on the original input image, which serves as the ground truth for the generator. (c) represents the outcome of image enhancement through the utilization of the adversarial network, which involves



**Fig. 4.** The output images of each stage of the proposed model: (a) the original input image, (b) the LL subband image after discrete wavelet transform and normalization, (c) the enhanced image using image enhancement method, (d) the binarization image using the method combining local and global features, (e) the ground truth image.

the removal of the background color and highlighting the text color. (d) is the final output image by using the proposed method, which demonstrates the close proximity of our result to the ground truth image (e).

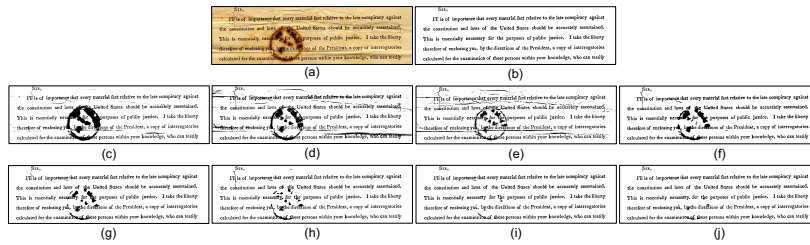


**Fig. 5.** Examples of document image binarization for the input image PR16 of DIBCO 2013 dataset by different methods: (a) original input images, (b) the ground truth, (c) Otsu [18], (d) Niblack [17], (e) Sauvola [26], (f) Vo [32], (g) He [10], (h) Zhao [33], (i) Suh [28], (j) Ours.

**Table 3.** Quantitative comparison (FM/p-FM/PSNR/DRD) with other state-of-the-art models for document image binarization on benchmark datasets. Best and 2nd best performance are in red and blue colors, respectively.

(a) DIBCO 2011					(b) H-DIBCO 2016				
Methods	FM↑	p-FM↑	PSNR↑	DRD↓	Methods	FM↑	p-FM↑	PSNR↑	DRD↓
Niblack [17]	70.44	73.03	12.39	24.95	Sauvola [26]	84.27	89.10	17.15	6.09
1st Place [20]	80.86	\	16.13	5.36	Otsu [18]	86.59	89.92	17.79	5.58
Otsu [18]	82.10	85.96	15.72	8.95	1st Place [23]	87.61	91.28	18.11	5.21
Sauvola [26]	82.35	88.63	15.75	7.86	Guo [9]	88.51	90.46	18.42	4.13
He [10]	91.92	95.82	19.49	2.37	Zhao [33]	89.77	94.85	18.80	3.85
Vo [32]	92.58	94.67	19.16	2.38	Vo [32]	90.01	93.44	18.74	3.91
Zhao [33]	92.62	95.38	19.58	2.55	Bera [2]	90.43	91.66	18.94	3.51
Suh [28]	93.57	95.93	20.22	1.99	He [10]	91.19	95.74	19.51	3.02
Tensmeyer [31]	93.60	97.70	20.11	1.85	Suh [28]	92.24	95.95	19.93	2.77
Ours	94.08	97.08	20.51	1.75	Ours	91.46	96.32	19.66	2.94

(c) DIBCO 2013					(d) DIBCO 2017				
Methods	FM↑	p-FM↑	PSNR↑	DRD↓	Methods	FM↑	p-FM↑	PSNR↑	DRD↓
Niblack [17]	71.38	73.17	13.54	23.10	Otsu [18]	77.73	77.89	13.85	15.54
Otsu [18]	80.04	83.43	16.63	10.98	Sauvola [26]	77.11	84.10	14.25	8.85
Sauvola [26]	82.73	88.37	16.98	7.34	Bera [2]	83.38	89.43	15.45	6.71
Vo [32]	93.43	95.34	20.82	2.26	Jemni [13]	89.80	89.95	17.45	4.03
He [10]	93.36	96.70	20.88	2.15	Zhao [33]	90.73	92.58	17.83	3.58
Zhao [33]	93.86	96.47	21.53	2.32	1st Place [24]	91.04	92.86	18.28	3.40
1st Place [22]	92.12	94.19	20.68	3.10	Kang [14]	91.57	93.55	15.85	2.92
Ours	95.24	97.51	22.27	1.59	Ours	90.95	93.79	18.57	2.94

## 4.6 Experimental Results

This work evaluates various models on four datasets: DIBCO 2011, DIBCO 2013, H-DIBCO 2016, and DIBCO 2017. Due to the lack of optical character recognition (OCR) result in dataset, both the proposed method and other SOTA methods are evaluated using the four evaluation metrics described in Section 4.2. The evaluation results on the benchmark datasets are presented in Table 3. Our proposed method achieves the best performance in FM, PSNR, and DRD value on DIBCO 2011 dataset, with a close approximation in p-FM (97.08) to the highest performance (97.70). Moreover, the proposed method attains the highest performance across all evaluation metrics on DIBCO 2013 dataset. For the rest DIBCO datasets, the proposed method consistently ranks within the top two for four evaluation metrics. These results demonstrate that the proposed method outperforms other SOTA methods for image binarization of color degraded documents.

## 5 Conclusion and Future Work

To perform image binarization on color degraded documents, this work splits the RGB three-channel input image into three single-channel images, and train the adversarial network on each single-channel image, respectively. Moreover,

this work performs DWT on  $224 \times 224$  patches of single-channel image in the image preprocessing stage to improve the model performance. We name the proposed generative adversarial network as CCDWT-GAN, which achieves SOTA performance on multiple benchmark datasets.

Furthermore, our proposed method is compatible with various DWT and other backbone networks. It is worth noting that the Transformer architecture-based model has achieved impressive performance in computer vision tasks recently. For future work, our intention is to incorporate the self-attention mechanism into the generator to create a more efficient method, advancing the development of document image binarization.

## References

1. Bartusiak, E.R., Yarlagadda, S.K., Güera, D., Bestagini, P., Tubaro, S., Zhu, F.M., Delp, E.J.: Splicing detection and localization in satellite imagery using conditional gans. In: 2019 IEEE Conference on Multimedia Information Processing and Retrieval (MIPR). pp. 91–96. IEEE (2019)
2. Bera, S.K., Ghosh, S., Bhowmik, S., Sarkar, R., Nasipuri, M.: A non-parametric binarization method based on ensemble of clustering algorithms. *Multimedia Tools and Applications* **80**(5), 7653–7673 (2021)
3. Bhunia, A.K., Bhunia, A.K., Sain, A., Roy, P.P.: Improving document binarization via adversarial noise-texture augmentation. In: 2019 IEEE International Conference on Image Processing (ICIP). pp. 2721–2725. IEEE (2019)
4. De, R., Chakraborty, A., Sarkar, R.: Document image binarization using dual discriminator generative adversarial networks. *IEEE Signal Processing Letters* **27**, 1090–1094 (2020)
5. Deng, F., Wu, Z., Lu, Z., Brown, M.S.: Binarizationshop: a user-assisted software suite for converting old documents to black-and-white. In: Proceedings of the 10th annual joint conference on Digital libraries. pp. 255–258 (2010)
6. Gatos, B., Ntirogiannis, K., Pratikakis, I.: Icdar 2009 document image binarization contest (dibco 2009). In: 2009 10th International conference on document analysis and recognition. pp. 1375–1382. IEEE (2009)
7. Goodfellow, I., Pouget-Abadie, J., Mirza, M., Xu, B., Warde-Farley, D., Ozair, S., Courville, A., Bengio, Y.: Generative adversarial networks. *Communications of the ACM* **63**(11), 139–144 (2020)
8. Gulrajani, I., Ahmed, F., Arjovsky, M., Dumoulin, V., Courville, A.C.: Improved training of wasserstein gans. *Advances in neural information processing systems* **30** (2017)
9. Guo, J., He, C., Zhang, X.: Nonlinear edge-preserving diffusion with adaptive source for document images binarization. *Applied Mathematics and Computation* **351**, 8–22 (2019)
10. He, S., Schomaker, L.: Deepotsu: Document enhancement and binarization using iterative deep learning. *Pattern recognition* **91**, 379–390 (2019)
11. Hedjam, R., Cheriet, M.: Historical document image restoration using multispectral imaging system. *Pattern Recognition* **46**(8), 2297–2312 (2013)
12. Isola, P., Zhu, J.Y., Zhou, T., Efros, A.A.: Image-to-image translation with conditional adversarial networks. In: Proceedings of the IEEE conference on computer vision and pattern recognition. pp. 1125–1134 (2017)

13. Jemni, S.K., Souibgui, M.A., Kessentini, Y., Fornés, A.: Enhance to read better: a multi-task adversarial network for handwritten document image enhancement. *Pattern Recognition* **123**, 108370 (2022)
14. Kang, S., Iwana, B.K., Uchida, S.: Complex image processing with less data—document image binarization by integrating multiple pre-trained u-net modules. *Pattern Recognition* **109**, 107577 (2021)
15. Kligler, N., Katz, S., Tal, A.: Document enhancement using visibility detection. In: *Proceedings of the IEEE Conference on Computer Vision and Pattern Recognition*. pp. 2374–2382 (2018)
16. Nafchi, H.Z., Ayatollahi, S.M., Moghaddam, R.F., Cheriet, M.: An efficient ground truthing tool for binarization of historical manuscripts. In: *2013 12th International Conference on Document Analysis and Recognition*. pp. 807–811. IEEE (2013)
17. Niblack, W.: *An introduction to digital image processing*. Strandberg Publishing Company (1985)
18. Otsu, N.: A threshold selection method from gray-level histograms. *IEEE transactions on systems, man, and cybernetics* **9**(1), 62–66 (1979)
19. Pratikakis, I., Gatos, B., Ntirogiannis, K.: H-dibco 2010-handwritten document image binarization competition. In: *2010 12th International Conference on Frontiers in Handwriting Recognition*. pp. 727–732. IEEE (2010)
20. Pratikakis, I., Gatos, B., Ntirogiannis, K.: Icdar 2011 document image binarization contest (dibco 2011). In: *2011 International Conference on Document Analysis and Recognition*. pp. 1506–1510. IEEE (2011)
21. Pratikakis, I., Gatos, B., Ntirogiannis, K.: Icfhr 2012 competition on handwritten document image binarization (h-dibco 2012). In: *2012 international conference on frontiers in handwriting recognition*. pp. 817–822. IEEE (2012)
22. Pratikakis, I., Gatos, B., Ntirogiannis, K.: Icdar 2013 document image binarization contest (dibco 2013). In: *2013 12th International Conference on Document Analysis and Recognition*. pp. 1471–1476. IEEE (2013)
23. Pratikakis, I., Zagoris, K., Barlas, G., Gatos, B.: Icfhr2016 handwritten document image binarization contest (h-dibco 2016). In: *2016 15th International Conference on Frontiers in Handwriting Recognition (ICFHR)*. pp. 619–623. IEEE (2016)
24. Pratikakis, I., Zagoris, K., Barlas, G., Gatos, B.: Icdar2017 competition on document image binarization (dibco 2017). In: *2017 14th IAPR International Conference on Document Analysis and Recognition (ICDAR)*. vol. 1, pp. 1395–1403. IEEE (2017)
25. Ronneberger, O., Fischer, P., Brox, T.: U-net: Convolutional networks for biomedical image segmentation. In: *International Conference on Medical image computing and computer-assisted intervention*. pp. 234–241. Springer (2015)
26. Sauvola, J., Pietikäinen, M.: Adaptive document image binarization. *Pattern recognition* **33**(2), 225–236 (2000)
27. Suh, S., Kim, J., Lukowicz, P., Lee, Y.O.: Two-stage generative adversarial networks for document image binarization with color noise and background removal. *arXiv preprint arXiv:2010.10103* (2020)
28. Suh, S., Lee, H., Lukowicz, P., Lee, Y.O.: Cegan: Classification enhancement generative adversarial networks for unraveling data imbalance problems. *Neural Networks* **133**, 69–86 (2021)
29. Sulaiman, A., Omar, K., Nasrudin, M.F.: Degraded historical document binarization: A review on issues, challenges, techniques, and future directions. *Journal of Imaging* **5**(4), 48 (2019)
30. Tan, M., Le, Q.: Efficientnet: Rethinking model scaling for convolutional neural networks. In: *International conference on machine learning*. pp. 6105–6114 (2019)

31. Tensmeyer, C., Martinez, T.: Document image binarization with fully convolutional neural networks. In: 2017 14th IAPR international conference on document analysis and recognition (ICDAR). vol. 1, pp. 99–104. IEEE (2017)
32. Vo, Q.N., Kim, S.H., Yang, H.J., Lee, G.: Binarization of degraded document images based on hierarchical deep supervised network. *Pattern Recognition* **74**, 568–586 (2018)
33. Zhao, J., Shi, C., Jia, F., Wang, Y., Xiao, B.: Document image binarization with cascaded generators of conditional generative adversarial networks. *Pattern Recognition* **96**, 106968 (2019)
34. Zhou, Z., Siddiquee, M.M.R., Tajbakhsh, N., Liang, J.: Unet++: Redesigning skip connections to exploit multiscale features in image segmentation. *IEEE transactions on medical imaging* **39**(6), 1856–1867 (2019)